19th INTERNATIONAL CONGRESS ON ACOUSTICS
MADRID, 2-7 SEPTEMBER 2007

THE EFFECT OF HIFU-RELEVANT RATES OF HEATING ON THE GROWTH AND DISSOLUTION OF NUCLEI AVAILABLE FOR INERTIAL CAVITATION

PACS: 47.55.dd 47.55.dp 87.54.Hk

Webb, Ian R.[1]; Arora, Manish[1]; Collin, Jamie R.T.[1]; Payne, Stephen J.[1]; Roy, Ronald A.[2] and Coussios, Constantin-C.[1]

[1]Institute of Biomedical Engineering, Dept. of Engineering Science, University of Oxford, Oxford, OX1 3PJ, United Kingdom; ian.webb@eng.ox.ac.uk
[2]Dept. of Aerospace & Mechanical Engineering, Boston University, Boston, MA 02215, USA.

ABSTRACT

A theoretical model is sought to explain recent experimental results which have shown the sudden onset of inertial cavitation after a significant period of ultrasound insonation. It is thought that there initially exists a population of bubbles with sub-optimal radii for inertial cavitation, which grow during the insonation period to become nuclei within the optimal size range to cavitate inertially. Rectified diffusion during bubble oscillation, and the changes in the bubble nucleation environment and their subsequent dynamics caused by ultrasonic heating, are amongst the mechanisms that could be responsible for nuclei growth. In this work, the effects of elevating the temperature of the medium surrounding a bubble, resulting in higher vapour pressures and decreased solubility of gas in the bulk medium, is investigated. A single bubble model is formulated by coupling a numerical solution of the mass diffusion PDE and the Rayleigh-Plesset Equation, taking into account temperature dependence of surface tension, vapour pressure, Henry's constant and diffusion coefficient. It is shown that an increase in the temperature at HIFU-relevant heating rates is on its own not sufficient to increase the radii of sub-optimal bubbles into the optimal range for inertial cavitation to take place.

1. INTRODUCTION

The presence of inertial cavitation during HIFU exposures can be important in a clinical setting, for example, in the ablation of cancers, as controlled and sustained bubble activity can lead to greater rates of heating than achievable when heating is solely caused by ultrasound absorption [1,2]. If it were possible to control the location of the cavitating bubble cloud, treatment times could be substantially reduced. It is therefore necessary to know when inertial cavitation is likely to occur, as unexpected activity could lead to the destruction of healthy cells if an area is over-treated, or the bubbles reflect the incoming ultrasound and re-position the focus.

Apfel and Holland [3] showed that, at a particular frequency of ultrasound insonation, there exists a threshold pressure-radius curve above which inertial cavitation will occur. The curve exhibits a minimum for radii in the 0.1μm to 1μm range. This implies that, at a certain pressure amplitude, there is an optimal range of nuclei sizes that will inertially cavitate. However, this work only considers single-pulse ultrasound excitation, assuming the presence of a range of sizes of pre-existing nuclei in pure water, whilst in therapeutic ultrasound one has to deal with longer pulses in an environment that contains a limited range of nuclei sizes.

Church [4] expanded on the work of Apfel and Holland, looking at the effects of longer pulses of ultrasound in both water and blood. He showed that the cavitation threshold was reduced significantly as the number of acoustic cycles was increased, and that the threshold was higher in blood than water owing to the higher viscosity of blood, but did not go further to state the effect of a viscoelastic material such as human tissue. The optimal range of nuclei for cavitation in the Church model is not significantly different from that of Apfel and Holland.

It must be noted in the above studies that there are only two outcomes when the HIFU beam is switched on; either cavitation does not occur, or it does so within the first few acoustic cycles. This assumption has been contradicted by recent experimental results in low cavitation-threshold tissue-mimicking materials, which have shown the onset of inertial cavitation after many acoustic cycles. Examples include the results of Edson [1]; for a one second exposure at pressure amplitude close to threshold (1.8 MPa), cavitation activity is not seen when the ultrasound is first incident on the phantom but is apparent halfway through the exposure. Experiments in Oxford have also shown the onset on cavitation in tissue-mimicking phantoms half to three-quarters of the way through exposures of time-order of tens of seconds. These results are not immediately applicable to human tissue, which exhibits a much higher cavitation threshold.

It is thought that the sudden onset of inertial cavitation is caused by a change in the size range of the nuclei present. Initially, the bubbles present in the medium have radii that are sub-optimal for cavitation; during the insonation period the bubbles grow to become of an optimal size to inertially cavitate.

Rectified diffusion is one possible mechanism that could be responsible for the bubble growth during the insonation period; both Eller and Flynn [5] and Fyrillas and Szeri [6] present mathematical models of rectified diffusion at a single temperature. However, the increase in temperature caused by the ultrasonic heating will alter both the nucleation environment, nucleation threshold and the dynamics of the pre-existing bubbles present in the medium. The two important effects of elevated temperature – an increase in the vapour pressure and a decrease in the solubility of gas in the surrounding medium – will both tend to cause growth of pre-existing nuclei irrespective of whether there is a rectified diffusion process.

The single bubble model developed in the following section focuses on the growth or dissolution of pre-existing bubbles in a liquid undergoing heating in the absence of an ultrasound field, to establish whether an elevation in temperature alone is sufficient to increase the radii of small bubbles (< 1μm) to the optimal range for inertial cavitation. We neglect the effects of rectified diffusion in this model. In section 3, we show results from the model and establish that there exists a heating rate threshold for bubble growth that is related to the initial bubble size.

2. MATHEMATICAL FORMULATION AND METHODS

Single Bubble Model

A single bubble model is formulated in spherical coordinates to determine the bubble motion caused by a temperature elevation of the bulk liquid surrounding the bubble. It is assumed that the bubble is perfectly spherical at all times, and the temperature is spatially uniform across both liquid and the bubble contents. The Rayleigh-Plesset equation, (Eq. 1), is used as the equation of motion for the bubble; as there is no acoustic driving term and the growth of the bubble is relatively slow – over time periods of milliseconds to seconds – the contributions of the inertial terms are negligible. The Rayleigh-Plesset equation can then be reduced to the Laplace Equation, (Eq. 2), which equates the internal and external pressures acting on the bubble:

$$R\ddot{R} + \frac{3}{2}\dot{R}^2 = \frac{p_g + p_v - p_\infty}{\rho_L} - \frac{2\sigma}{\rho_L R} - \frac{4\nu_L \dot{R}}{R} \qquad (1)\,, \qquad p_g + p_v = p_\infty + \frac{2\sigma}{R} \qquad (2)$$

where R is the bubble radius, p_g the gas pressure within the bubble, p_v the vapour pressure within the bubble, p_∞ the ambient liquid pressure, σ the surface tension coefficient, ν_L the kinematic viscosity of the liquid, ρ_L the liquid density, and the dot notation used to denote differentiation with respect to time.

In this model, the ideal gas equation (Eq. 3) is used to define the relationship between the gas pressure, bubble volume (V), bubble mass (m) and temperature (T); R_g is the gas constant. The gas pressure in the Laplace Equation can therefore be related to a temperature variation $T(t)$ and the initial bubble conditions, represented by the '0' subscript (Eq. 4).

$$p_g V = m R_g T \qquad (3)\,, \qquad p_g = p_{g0}\frac{m}{m_0}\frac{R_0^3}{R^3}\frac{T(t)}{T_0} \qquad (4)$$

The Laplace Equation can then be rearranged into a cubic equation in R:

$$(p_\infty - p_v)R^3 + 2\sigma R^2 - p_{g0}R_0^3 \frac{m}{m_0}\frac{T(t)}{T_0} = 0 \qquad (5)$$

From the Laplace Equation (Eq. 2) it can be seen that the gas pressure p_g within the bubble will differ from the ambient pressure p_∞ within the liquid, resulting in a pressure gradient across the bubble wall. This drives a mass diffusion process, causing the bubble to grow or dissolve dependent on the direction of the gradient. At t = 0, for all bubble sizes, the gas pressure within the bubble is greater than that in the liquid, owing to the surface tension term, and mass flows out of the bubble. The diffusion process must be incorporated within the bubble model.

The diffusion equation in spherical coordinates is given by

$$\frac{\partial \rho}{\partial t} = \frac{D}{r^2}\left[\frac{\partial}{\partial r}\left(r^2 \frac{\partial \rho}{\partial r}\right)\right] \qquad (6)$$

where ρ represents gas concentration, D is the diffusion coefficient and r the radial coordinate. The convective term in the diffusion equation has been neglected; owing to the slow variation of the bubble radius the relative contribution of this term will be negligible.

To set the boundary conditions of the diffusion equation, a diffusion layer is defined around the bubble with its maximum radius at L. At the outer boundary, the mass concentration is equal to the initial bulk concentration ρ_i, which is assumed to be the saturation concentration of that species in water at 20 ºC. The mass concentration in the bulk medium outside of the diffusion layer is assumed to be static; any temperature increase will supersaturate the solution but the gas cannot move anywhere unless the gradient is favourable. The inner boundary condition is set by Henry's Law (7), which relates the partial pressure of the gas within the bubble to the mass concentration of that species in the liquid at the bubble.

$$\rho_w = p_g H \qquad \text{at} \qquad r = R \qquad (7)$$

The rate of mass diffusing into or out of the bubble is then given as:

$$\dot{m} = 4\pi R^2 D(T)\left.\frac{\partial \rho}{\partial r}\right|_{r=R} \qquad (8)$$

As we are concerned with the growth or dissolution of the bubble induced by a change in the temperature of the bulk medium, the temperature dependent variation of the parameters in the above equations must be defined. Surface tension σ, vapour pressure p_v, diffusion coefficient D and Henry's constant H need to be considered. The approximate nature of these dependencies for an oxygen bubble in water is given by Eqs. (9) to (11); the variation of vapour pressure with temperature is assumed linear in this work. T_c is a critical temperature and its numerical value is given in Table I.

$$\sigma = 0.2358\tau^{1.256}(1 - 0.625\tau) \quad \text{where} \quad \tau = 1 - \frac{T}{T_c} \qquad (9)$$

$$H(T) = 1.385\times10^{-9}\exp\left(\frac{1700}{T}\right) \qquad (10), \qquad D(T) = 3.39\times10^{-6}\exp\left(-\frac{2183}{T}\right) \qquad (11)$$

To complete the model, we define a relevant time-temperature profile. On timescales that are short relative to the thermal diffusion timescale, the effects of conduction of heat away from the bubble are negligible and a linear relation between temperature and time exists (Eq. 12). When conduction does have an effect, Newton's Law of Cooling provides an approximate model, and the temperature profile takes the form of Eq (13). Both t_{rise} and τ_c are time constants. Eq. 13 will be referred to as the 'exponential profile'; both profiles will be investigated in this work.

$$T(t) = T_0 + T_{rise}\frac{t}{t_{rise}}, \quad t \le t_{rise} \qquad (12), \qquad T(t) = T_0 + T_{rise}\left[1 - \exp\left(-\frac{t}{\tau_c}\right)\right] \qquad (13)$$

Numerical Methods

To ascertain whether sub-optimal bubbles can reach an optimal size for inertial cavitation, it is necessary to compute the radius-time (*R-t*) curve that results from the solution of the above set of equations. This computation is complicated by their highly coupled nature – the boundary condition of the diffusion equation is dependent upon the solution of the equation of motion, which itself is dependent on the amount of gas entering the bubble and hence the diffusion equation. No known analytical solution is known to such a problem, hence it is necessary to employ a numerical method to compute the *R-t* curve.

A finite difference scheme is implemented to solve the diffusion equation across the spatial grid at each timestep, using the Crank-Nicolson method [7] for added stability and accuracy in the computation. The initial condition on the concentration field is taken to be the solution of Eq. (6) when the bubble is at equilibrium, i.e. with the temporal derivative set to zero. Once the concentration field has been computed, the rate of change of spatial concentration at the bubble wall is used to find the amount of mass entering the bubble. Taking into account this change in mass, the new bubble radius and gas pressure is calculated using Eq. (5) and the Laplace Equation, Eq. (2), giving the new boundary conditions for the next timestep of the diffusion equation solution.

Further complications arise owing to the fact a boundary condition is being imposed on a moving boundary. Secondly, the area of interest in the solution of the diffusion equation, namely the part adjacent to the bubble, shows the greatest rate of change of concentration and hence is more prone to numerical inaccuracies when a uniformly spaced grid is used. To overcome this, the co-ordinate transformation of Eq. (14) is implemented, fixing the bubble boundary at *y*=0 and redistributing the spatial grid so that the density of grid points is greater where the concentration is changing faster, i.e. near the bubble wall. In this work, *n*=10 is chosen, giving sufficient spatial resolution at the bubble wall.

$$y = \ln\left(\alpha r^{1/n} + \beta\right) \tag{14}$$

where

$$\alpha = \frac{\mathrm{e} - 1}{L^{1/n} - R^{1/n}} \quad , \quad \beta = \frac{L^{1/n} - \mathrm{e}\, R^{1/n}}{L^{1/n} - R^{1/n}} \tag{15}$$

Parameter Values

The numerical simulations were based on the response of an oxygen bubble in water, which resulted in simplified calculations relative to working with an air bubble. The similarity of both the diffusion coefficient in water and Henry's constant of oxygen to those parameters for air, of which oxygen is a major constituent, allowed this simplification to be made. Table I lists the parameter values from the above equations; during the iterations a time step of 0.1 ms and a spatial step of 0.01 in the transformed (y) co-ordinate system were used.

Table I – Numerical Simulation Parameter Values

Parameter	Value	Parameter	Value
L	0.01 m	p_v (293 K)	2.34 kPa
T_0	293 K	p_v (333 K)	19.92 kPa
T_{final}	333 K	p_∞	101.325 kPa
T_{rise}	40 K	ρ_L	1000 kgm^{-3}
T_c	647.1 K	R_g	259.8 $Jkg^{-1}K^{-1}$

3. RESULTS AND DISCUSSION

Figure 1 shows the *R-t* curves produced by the model for two different bubble sizes, using both the linear and exponential heating profiles. In each case the total temperature rise is 40K; the time constant τ_c for the exponential profile is chosen so that the areas under the temperature-

time graphs, and hence the thermal dose, is identical in both cases. This gives an initial heating rate for the exponential curve that is twice as fast as for the linear rise.

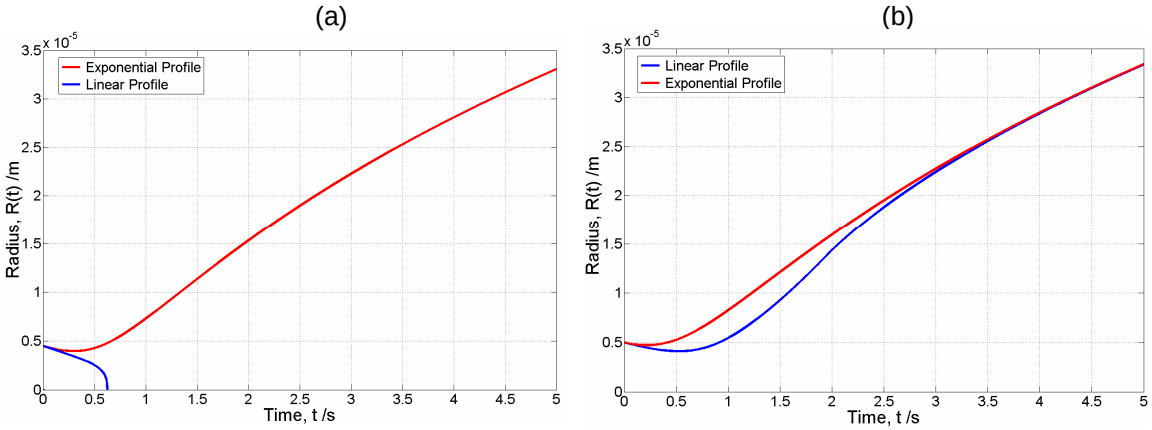

Figure 1 – Radius-time curves for a 4.5 μm bubble (a) and a 5 μm bubble (b). Time constants for the temperature-time profiles are t_{rise} = 2 s (linear) and τ_c = 1 s (exponential)

It is clear that the initial rate of heating is key to bubble growth or dissolution; for the 4.5 μm bubble of Fig 1 (a), the slower, linear heating profile results in bubble dissolution whereas the faster, exponential heating profile results in bubble growth. Note that without any imposed temperature elevation, bubbles will dissolve. However, if a temperature rise results in bubble growth, then the resultant *R-t* profile (as *t* tends to infinity) is independent of the temperature profile (Fig. 1 (b)). Here, the controlling factor is the thermal dose, proportional to the area under the Temperature-time curve, which is identical for both the linear and exponential profile.

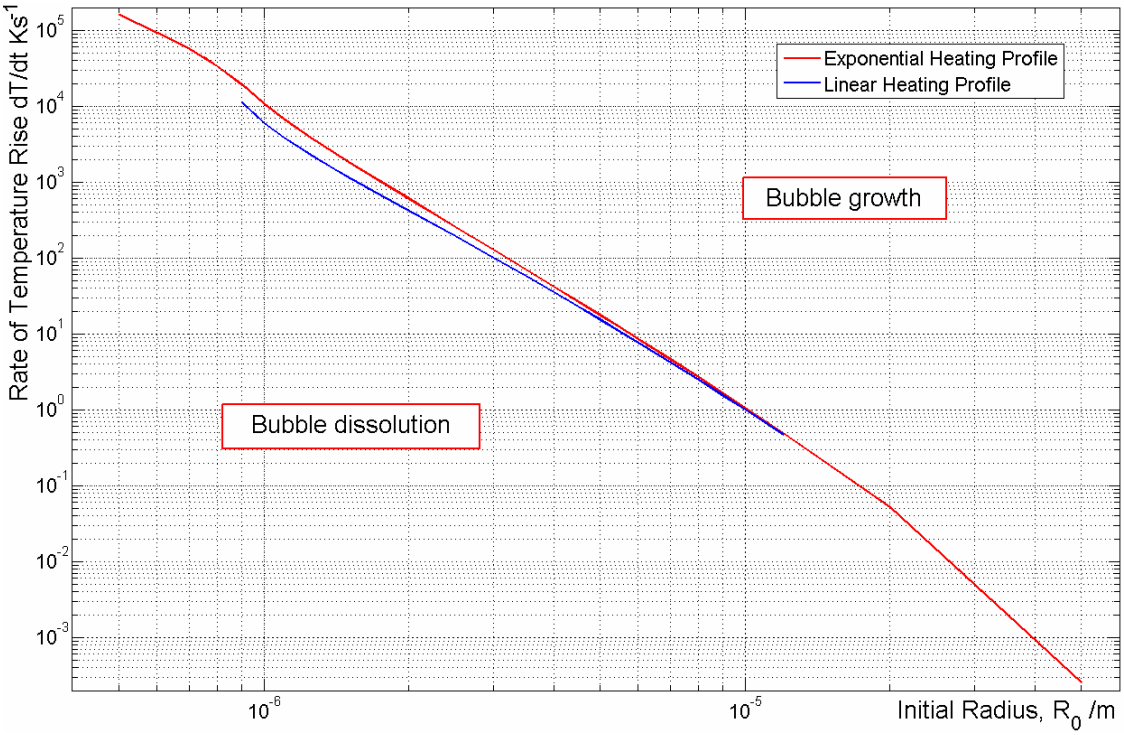

Figure 2 – Threshold Rates of Heating for various radii bubbles (0.5 μm to 50 μm) for both exponential (red) and linear (blue) rates of heating

Figure 2 shows a threshold rate of heating exists for bubble growth dependent on initial bubble size. We are primarily concerned with rates of heating relevant to HIFU treatment, which will not exceed 100 Ks^{-1}. Bubble growth will therefore occur for bubbles greater than 3 μm in size. The heating profile (linear or exponential) used in the model has little, if any effect on this result. In the 0.1-1μm size range - the optimal range suggested by Apfel and Holland, and by Church – the rates of heating required to overcome the effects of high surface tension pressures are very

large. In these cases the very short time periods involved have some effect on the numerical accuracy of the results obtained and the validity of the “slow growth” assumption. It can, however, be said with some certainty that in water, sub-optimal bubbles cannot grow to become nuclei optimal for cavitation solely under the effects of heating, neglecting rectified diffusion.

Model Limitations

There are several limitations to the model presented. Importantly, the oxygen-in-water model does not describe bubble dynamics in tissue explicitly. However, the fact that sub-optimal bubbles will not grow under heating is likely to hold true for any surrounding medium with a greater viscosity or compressibility than water, as the greater damping and/or resistive elastic forces will impede bubble growth more than the surface tension of water alone.

The assumed linear variation of vapour pressure with temperature can be shown to lead to slight over-estimates of the actual bubble radius over time, and hence gives an underestimate of the threshold rate of heating necessary for a bubble to grow. A more accurate model would therefore only reinforce the conclusion that bubble growth under HIFU-relevant heating rates alone is highly unlikely.

Although a common occurrence in previous works, the validity of the diffusion layer (or thin-boundary layer) assumption has been challenged [8]. For this model, changing the size of the diffusion layer above the 10mm used in the model alters the *R-t* curves obtained by less than 0.2%; reduction to 1mm alters the response by less than 1% over the first 5 seconds of the *R-t* curve. The small differences in the model output indicate that the diffusion layer assumption is accurate for a single bubble in an infinite extent of liquid over the time periods in question.

4. CONCLUSIONS

In this work a single bubble model has been developed to simulate the radius-time profile of a gas bubble undergoing an increase in temperature at HIFU-relevant heating rates. The initial pressure gradient, and hence the gas concentration gradient, is such that all bubbles will partially dissolve at the beginning of the heating period. If the rate of heating lies above a certain radius-dependent threshold then the concentration gradient reverses, mass diffuses into the bubble and bubble growth results. When bubble growth is induced by the temperature increase, the steady-state radius is dependent on the thermal dose and not the imposed temperature profile. However, if bubbles that are too small to inertially cavitate are to grow, a far greater rate of heating, approximately 10,000 Ks^{-1}, is required than it is possible to deliver using HIFU. We can therefore conclude that heating alone, in the absence of an ultrasound field, is not sufficient to increase the radius of nuclei that are sub-optimal for cavitation into the optimal range. Either another mechanism, such as rectified diffusion, is partially or wholly responsible for the bubble growth necessary for cavitation to take place, or there is a significant change in the nucleation threshold caused by the increase in temperature during HIFU exposure which allows the nucleation of bubbles within the optimal size range for inertial cavitation. The investigation of these factors will form the basis for future work in this area.

References: [1] P.L. Edson: The role of acoustic cavitation in enhanced ultrasound-induced heating in a tissue-mimicking phantom. Ph.D. dissertation, Boston University, 2001.
[2] C.R. Thomas, C.H. Farny, C.C. Coussios, R.A. Roy and R.G. Holt: Dynamics and control of cavitation during high-intensity focussed ultrasound application. ARLO **6, No. 3** (2005) 182-187
[3] R.E. Apfel and C.K. Holland: Gauging the likelihood of cavitation from short-pulse, low-duty cycle diagnostic ultrasound. Ultrasound in Medicine and Biology **17, No.2** (1990) 179-185
[4] C.C. Church: Frequency, pulse length and the mechanical index. Acoustic Research Letters Online **6, No. 3**, (2005) 162-168
[5] A. Eller and H.G. Flynn: Rectified Diffusion during Nonlinear Pulsations of Cavitation Bubbles. Journal of the Acoustical Society of America **37** (1965), 493-503
[6] M.M. Fyrillas and A.J. Szeri: Dissolution or growth of soluble spherical oscillating bubbles. Journal of Fluid Mechanics **277** (1994) 381-407
[7] W.H. Press, S.A. Teukolsky, W.T. Vetterling and B.P. Flannery: Numerical Recipes in C++: The Art of Scientific Computing. Cambridge University Press, 2nd edition (2002) 849-953
[8] D.C. Venerus and N. Yala: Transport Analysis of Diffusion-Induced Bubble Growth and Collapse in Viscous Liquids. AIChE Journal **43, No. 11** (1997) 2948-2959